Microchemical Journal 207 (2024) 111939

Contents lists available at ScienceDirect

Microchemical Journal

journal homepage: www.elsevier.com/locate/microc

New electrochemiluminescent sensing platform based on SnS_2 for direct determination of citrulline

Claudia Martínez-Asenjo [a], Marcos Pita [b], Antonio L. De Lacey [b], Cristina Gutiérrez-Sánchez [a,c,*], Encarnación Lorenzo [a,c,d,*]

[a] Departamento de Química Analítica y Análisis Instrumental, Universidad Autónoma de Madrid, Madrid 28049, Spain
[b] Instituto de Catálisis y Petroleoquímica, CSIC, c/Marie Curie 2, L10, 28049 Madrid, Spain
[c] Institute for Advanced Research in Chemical Sciences (IAdChem), Universidad Autónoma de Madrid, Ciudad Universitaria de Cantoblanco, Madrid 28049, Spain
[d] IMDEA-Nanociencia, Ciudad Universitaria de Cantoblanco, Madrid 28049, Spain

ARTICLE INFO

Keywords:
Electrochemiluminescence sensing
Tin (IV) disulfide (SnS_2)
Gold nanoparticles
Citrulline
Sensor

ABSTRACT

Citrulline is a non-essential amino acid involved in the urea cycle and in the production of nitric oxide in many biological systems, therefore its detection and quantification are crucial for the diagnosis and treatment of various diseases. Citrulline is found in organisms, as it is an intermediate in the synthesis of the amino acid arginine, or by dietary intake.

In the present work we have developed an electrochemiluminescent sensor for the sensitive determination of citrulline, in which the compound is simultaneously as the analyte and the co-reactant in combination with a nanomaterial, SnS_2. The use of SnS_2 produces a considerable improvement in the electrochemiluminescent response when $[Ru(bpy)_3]^{2+}$ complex is used as luminophore.

After optimizing the parameters that influence the electrochemiluminescent response, a good linearity (R^2 = 0.998) was found in the range 10 μM–1 mM citrulline, with detection and quantification limits of 2.95 μM and 9.83 μM, respectively. Sensor's stability and durability studies were carried out and the potentially interfering compounds were analysed. The citrulline content was determined in a food sample, confirming the developed electrochemiluminescent sensor's viability.

1. Introduction

Citrulline is an α-amino acid organic compound belonging to the group of non-protein amino acids with a very specific metabolism in mammals. It was identified and isolated for the first time in watermelon juice [1]. Citrulline is synthesized exclusively in the intestine from glutamine. It is the main precursor of arginine, so its determination serves as an indicator about existing failures in the intestine of critically ill patients [2]. The transformation of citrulline to arginine occurs essentially in the kidneys, so irregularities in the metabolism of citrulline may indicate kidney problems and by enhancing nitric oxide production, plasma citrulline concentrations increase, and the risk of pulmonary hypertension decreases [1]. In patients suffering from sickle cell disease, citrulline has a vasodilator and antihypertensive effect. In addition, citrulline participates in the urea cycle and its accumulation or deficiency causes disorders, being able to reach lethality due to the increase in ammonia concentration [3]. Citrulline is capable of stimulating protein synthesis, without its absorption by the intestine or liver [4]. Hence, it is administered as a supplement orally as the intestine absorbs it better than arginine. It is used as an alternative to arginine and ornithine, since these ones convey side effects [1]. Citrulline is also found in a variety of foods, including almonds, cocoa, garlic, onion, peanuts, mushrooms, and some fish, such as salmon [5,6]. These foods have citrulline concentrations that are negligible compared to that present in watermelon [7].

Due to the importance of citrulline in metabolism and its beneficial effects, either through ingestion through food or through supplements, it is interesting to dispose of methods for its easy and accurate determination. Some works on its determination can be found in the literature based on surface-enhanced Raman spectroscopy [8], fluorescence spectroscopy [9,10], colorimetric method with logic gate behavior [11], high performance liquid chromatography with electrochemical detection [12] and electrochemical [13]. Most of these methods are time consuming or are not suitable for use in automatic systems. Thus, to

* Corresponding authors at: Departamento de Química Analítica y Análisis Instrumental, Universidad Autónoma de Madrid, Madrid 28049, Spain.
E-mail addresses: cristina.gutierrezs@uam.es (C. Gutiérrez-Sánchez), encarnacion.lorenzo@uam.es (E. Lorenzo).

https://doi.org/10.1016/j.microc.2024.111939
Received 9 July 2024; Received in revised form 20 September 2024; Accepted 14 October 2024
Available online 18 October 2024

develop new sensors that meet current demands fast response, simple, low cost, sensitive, miniaturized and are industrially scalable, focused on its detection and quantification is of great interest. However, to the best of our knowledge, the development of electrochemiluminescent sensors for the determination of citrulline is not underway.

Electrochemiluminescence (ECL) is an analytical technique in which electrochemistry and luminescence are combined. ECL is a technique based on the emission of light as a result of consecutive electrochemical reactions. In this process, intermediate species are obtained capable of participating in charge transfer reactions and generating excited states that, when returning to the ground state, emit light [14]. In this work, ECL is explored through a co-reactant pathway. The main components of the system are the luminophore and the co-reactant [15]. Luminophores are the light-emitting species and the luminophore par excellence is the inorganic complex tris(2,2′-bipyridyl)ruthenium(II), $[Ru(bpy)_3]^{2+}$. This complex presents a high luminescence and is capable of undergoing reversible electron transfer reactions [16]. The co-reactant is a chemical reagent that is oxidized or reduced on the electrode surface, generating intermediate species that yield highly reactive radicals. It has been described that the presence of amino groups and hydroxyl groups in a compound favor its use as a co-reactant, since these groups have a high electron exchange capacity [17]. In this work we explored the possibility that citrulline, in addition to be the analyte, acts as a co-reactant. Due to its chemical structure, citrulline is expected to be capable of acting as a co-reactant, therefore an electrochemiluminescent sensor has been developed for its detection.

It has been described that the use of nanomaterials can produce an improvement in the electrochemiluminescent response, since these, in addition to nanostructuring the surface of the electrodes, facilitate and accelerate charge transfer enabling the development of electrochemiluminescent sensors with greater sensitivity and lower detection limits [18–23]. In this sense, metallic nanoparticles have excellent optical, catalytic, magnetic and electronic properties, low cytotoxicity and high affinity with biomolecules [24]. Based on these properties, different ECL-based sensors employing gold nanoparticles (AuNPs) have been developed [25–27]. Semiconductor nanomaterials such as MoS_2 [28], Al_2O_3 [29], quantum dots [30,31] or α-germanium [32] have also been used with excellent results since the semiconductor nanoparticles can be electrochemically excited to generate their reduced or oxidized states, which subsequently can react with some co-reactants to produce electrochemiluminescent signals. Other semiconductor nanomaterials have not been exploited yet in the development of this kind of sensors but can have a great role by improving the final performance of these devices. In particular, SnS_2 is a nanomaterial that in its most stable and simplest structure, the polytype 2H, has a bandgap Eg = 2.2 eV. Its interesting electrical and optical characteristics [33] make it an excellent candidate for various applications such as batteries, gas sensors or photocatalysts. SnS_2 presents the energy at which the valence band is located could favor oxidative catalysis of the luminophore [34]. In addition, due to its high surface area, it provides a large number of active sites that could promote electron transfer at the electrode surface. However, in spite of the excellent properties of SnS_2 it has not been employed yet in the development of electrochemiluminescent sensors. In the present work, we demonstrate the applicability of SnS_2 in the development of very sensitive ECL sensors.

2. Experimental

Chemicals and instrumentation employed in this work, as well as the experimental procedures are described in detail in the Supplementary material.

3. Results and discussion

3.1. Development of the electrochemiluminescent citrulline sensing platform

The first step for the development of an electrochemiluminescent citrulline sensor is to check if citrulline acts as a co-reactant. To this end, the electrochemiluminescent response of the luminophore, the inorganic complex, $[Ru(bpy)_3]^{2+}$, was analyzed in the absence and in the presence of citrulline at SPCE (Fig. 1A) and SPAuE (Fig. 1B).

In Fig. 1 can be seen that in both platforms citrulline acted as a co-reactant, since the electrochemiluminescent signal obtained in the presence of citrulline and $[Ru(bpy)_3]^{2+}$ was considerably higher than that obtained individually. The increase in the electrochemiluminescent response is remarkable and is independent of the electrode used. Both citrulline and $[Ru(bpy)_3]^{2+}$ are oxidized by the potential sweep applied at the electrode. Citrulline gives rise to a radical intermediate species, capable of transferring an electron to the oxidized ruthenium complex. The formation of the $[Ru(bpy)_3]^{2+\bullet}$ species enables the regeneration of the initial $[Ru(bpy)_3]^{2+}$ through the release of accumulated energy in the form of light. This proposed process is reflected in the Scheme 1.

Fig. 1 shows the electrochemiluminescent increase (ΔECL) that is, the difference between the electrochemiluminescent signal produced by the luminophore $[Ru(bpy)_3]^{2+}$ by itself and the electrochemiluminescent signal that it is produced in the presence of citrulline as co-reactant. The higher the ΔECL, the greater the sensitivity and the lower the detection limit are expected for the citrulline sensor. Fig. 1 shows a higher ΔECL for SPAuE, a fact that can be attributed to the optical properties of gold and its excellent electrical conductivity, in addition to its high surface/volume ratio. Therefore, the SPAuE was selected as the working electrode for all subsequent experiments.

3.2. Characterization of SnS_2 synthesized

The SnS_2 is a semiconductor nanomaterial with a band gap energy of around 2.2 eV and has high resistance to photocorrosion and the energy at which the valence band is located could favor the oxidative catalysis of the luminophore. The ground level at which holes occur upon photoexciting SnS_2 provides a driving force that allows the luminophore to overcome the irreversibility of its natural oxidation catalytic activity. In addition, SnS_2 increases the active surface of the electrode, so a greater amount of citrulline and luminophore molecules can be oxidized. Thus, the emitted light is multiplied.

Previous literature describes that the use of semiconductor nanomaterials improves the electrochemiluminescent signal due to an increase in electron transfer. Another property of semiconductors is a broad bandgap energy and a high excitation binding energy. Semiconductor nanomaterials such as ZnO [35], quantum dots [36] MoS_2 [37] or α-Ge [32] are excellent candidates for improving electrochemiluminescent performance. Therefore, the effect of modifying the SPAuE with SnS_2 was explored. First of all, SnS_2 was synthesized as described in the experimental section 2.3 Procedures of the Supplementary material. Next, the synthesized SnS_2 was characterized using different techniques such as UV–visible spectroscopy, transmission electron microscopy with energy dispersive X-ray spectroscopy (TEM-EDX), DLS and zeta potential.

The absorption spectrum was recorded from 200 to 800 nm of a dispersion of SnS_2 in EtOH at a concentration of 0.10 mg/mL (Fig. S1). It can be seen that in the spectrum there is a maximum at 277 nm associated with SnS_2. It has been described in the bibliography that the absorbance spectrum of this nanomaterial presents variations in this absorption band depending on the temperature at which it was synthesized and the particle size. The intensity of absorption is determined by the synthesis temperature [38], being more intense the higher it is. The SnS_2 used in this work was synthesized at 180 °C [39], causing the absorption intensity not to be very high. The wavelength at which SnS_2

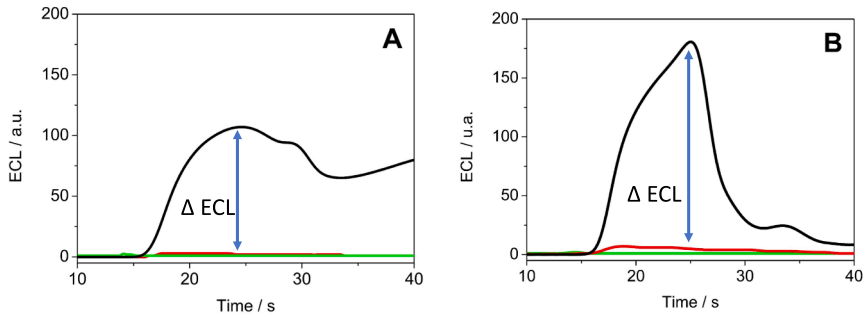

Fig. 1. ECL response versus time on A) SPCE and B) SPAuE for a 2 mM solution of $[Ru(bpy)_3]^{2+}$ (red line), 500 μM citrulline (green line) and a mixed solution containing 2 mM of $[Ru(bpy)_3]^{2+}$ and 500 μM citrulline (black line), both in 0.1 M PB, pH 8.0. A cyclic sweep was performed between 0 and 1.5 V at 50 mV/s. (For interpretation of the references to color in this figure legend, the reader is referred to the web version of this article.)

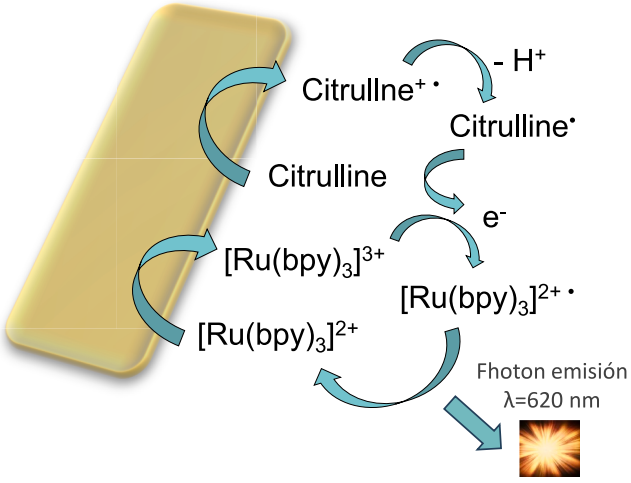

Scheme 1. Proposed electrochemiluminescent reaction mechanism that take place between the luminophore and the co-reactant on the electrode surface.

absorbs is influenced by the particle size [40].

Transmission electron microscopy (TEM) characterization was done to determine the morphology and size of the SnS_2. TEM allows a study at the structural level of SnS_2 crystals. Fig. 2a, b and d show a series of hexagonal SnS_2 crystals that overlap each other. The light and dark areas give an idea of the thickness of this nanomaterial, with lateral dimensions between 400 and 500 nm. In the EDX spectrum of Fig. 2c, the peaks corresponding to sulfur and tin are identified, showing that the synthesis of SnS_2 has been carried out successfully.

We also performed a Dynamic Light Scattering (DLS) characterization of SnS_2, since it provides information about the size of the particles (Fig. S2A) and the zeta potential, which is a measure of the magnitude of the electrostatic charge repulsion or attraction between the particles (Fig. S2B). The size distribution of SnS_2 crystals is shown in Fig. S2A. The particle size was observed to range from 710 to 1280 nm. This can be attributed to the presence of aggregates in the sample, as they scatter the light with much higher intensity. The agglomeration effect makes it difficult to obtain high-quality information, since the less intense scattering from smaller crystals is masked, resulting in broader and less precise peaks. Fig. S2B shows the result of the zeta potential value, a maximum of –22.43 mV was obtained, which suggests that the value of the electrostatic potential in the electrical double layer that forms around the crystals is negative. This could be associated with the negative charge of the sulfur at the edge of the structure. In addition, this parameter provides information on the stability of the dispersion under analysis, being able to classify it as stable dispersion (zeta potential in the range ±20–±30 mV) [41].

Once verified through exhaustive characterization that SnS_2 was correctly synthesized, SPAuE was modified with SnS_2 to be employed as an electrochemiluminescence platform and the influence of SnS_2 on the electrochemiluminescent response was studied.

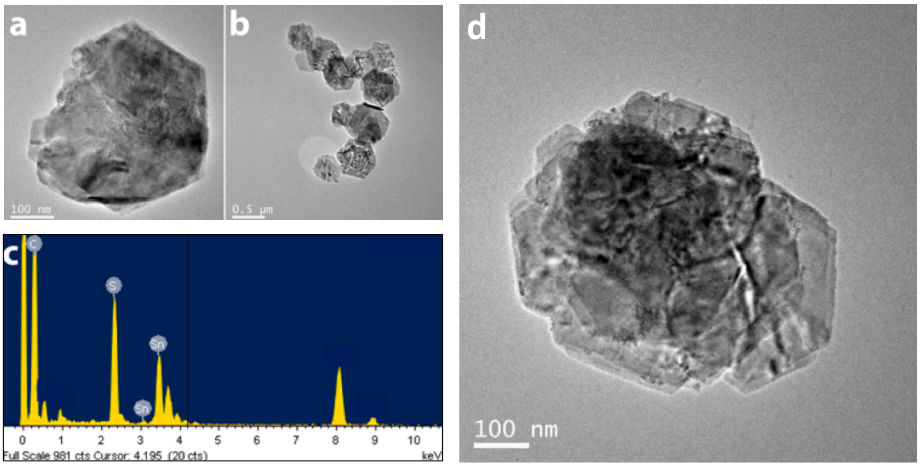

Fig. 2. A), b) and d) tem images obtained at different magnifications of sns_2 crystals. c) EDX spectrum of SnS_2.

3.3. Characterization of the modified SnS_2/SPAuE

The SnS_2-modified electrode has been characterized by different techniques. Electrochemical impedance spectroscopy (EIS) analysis has been carried out to study the interfacial properties of the surface, using ferrocyanide/ferricyanide (10 mM:10 mM) as redox probe in a 0.1 M PB, 0.1 M KCl, pH 7.0. The response of unmodified SPAuE and modified SPAuE with 5 μL of 0.10 mg/mL SnS_2 in EtOH (SnS_2/SPAuE) was studied.

Fig. S3A shows the Nyquist diagrams obtained for the unmodified electrode (SPAuE) and for the modified electrode (SnS_2/SPAuE). After electrode modification with SnS_2, there was an increase in resistance to charge transfer (RCT) from 13.8 Ω (SPAuE) to 59.3 Ω (SnS_2/SPAuE), suggesting that the modified electrode is less conductive. This was the expected result, since a conductive gold surface has been modified with a semiconductor nanomaterial.

In addition, the voltammograms of the redox probe at SPAuE and SnS_2/SPAuE were recorded (Fig. S3B). A decrease in peak current intensities was observed in the case of the electrode modified with 5 μL of SnS_2 in EtOH, in addition to an increase of peak separation, indicating slower electron transfer kinetics and confirming the impedance results previously obtained.

The gold electrode has a well-defined electroactive area. By depositing the SnS_2 on the surface of the SPAuE, it is expected that it will decrease. To verify that this occurs, cyclic voltammetry was performed in 0.1 M H_2SO_4 in the absence and presence of SnS_2. The electroactive area of the gold electrode is directly related to the area contained in the cathodic peak associated with the first scan (reduction) of the voltammogram (Fig. S4). Once the SPAuE is modified with SnS_2, the intensity of the peak decreases. This result agrees with what was expected since by modifying the electrode with the SnS_2 dispersion, the surface of the SPAuE that was exposed was smaller. This experiment confirms that the electrode has been successfully modified with SnS_2.

The images obtained by scanning electron microscopy (SEM) allowed us to visualize the surface of the SPAuE modified with 5 μL of a 0.10 mg/mL SnS_2 dispersion in EtOH. Fig. S5A corresponds to the unmodified gold electrode. The SPAuE surface has a similar shape to gold nanoparticles, in the form of spheres of different sizes. The image of the gold electrode modified with SnS_2 is shown in Fig. S5B, in which, in addition to the spheres associated with the SPAuE, a series of stacked hexagonal-shaped sheets can be observed randomly distributed throughout the surface.

The chemical composition of the electrode surface was studied by combining scanning electron microscopy with energy dispersive X-ray spectroscopy (SEM-EDX). The spectra obtained for the unmodified and SnS_2 modified SPAuE are presented in Fig. S6A and Fig. S6B, respectively. Fig. 3A shows the area where the analysis was carried out marked with the number 22. Both spectra present the peaks corresponding to gold. Only in the electrode modified with SnS_2 do the characteristic peaks of tin and sulfur appear (Fig. S6B), confirming the correct synthesis of SnS_2 and that the SPAuE has been adequately modified.

Fig. 3 shows the mapping performed on the surface of the SnS_2/SPAuE. The blue color indicates the presence of gold (Fig. 3C) throughout the surface and in large quantities. Tin (red) and sulfur (yellow) are shown in Fig. 3D and Fig. 3E, respectively. It can be seen how these last two are present on the entire surface, although in a non-homogeneous way since the colors have different intensity in different areas of the image. The high concentration of sulfur and tin in a specific area is also seen in the image of Fig. 3B, which combines the aforementioned images. It shows a purple background (combination of the three colors) and an orange zone (mixture of yellow and red), where the SnS_2 is more concentrated, thus confirming the correct modification of the SPAuE with this nanomaterial.

Raman spectroscopy was used to characterize the SnS_2-modified electrode. Fig. S7 shows the spectra obtained for SPAuE and SnS_2/SPAuE, with the second electrode showing the band corresponding to tin (IV) disulfide at 314 cm^{-1} [42]. This result confirms that the electrode it is correctly modified with SnS_2, since the SPAuE does not show this band.

An additional experiment was carried out in order to understand the electrochemilumnescent response for SPAuE and SnS_2/SPAuE (Fig. S8). Citrulline alone is not capable of providing an electrochemiluminescent response, even in the presence of SnS_2. It only presents electrochemiluminescence in the presence of luminophore, indicating that citrulline can act as a coreactant of $[Ru(bpy)_3]^{2+}$ on both electrodes.

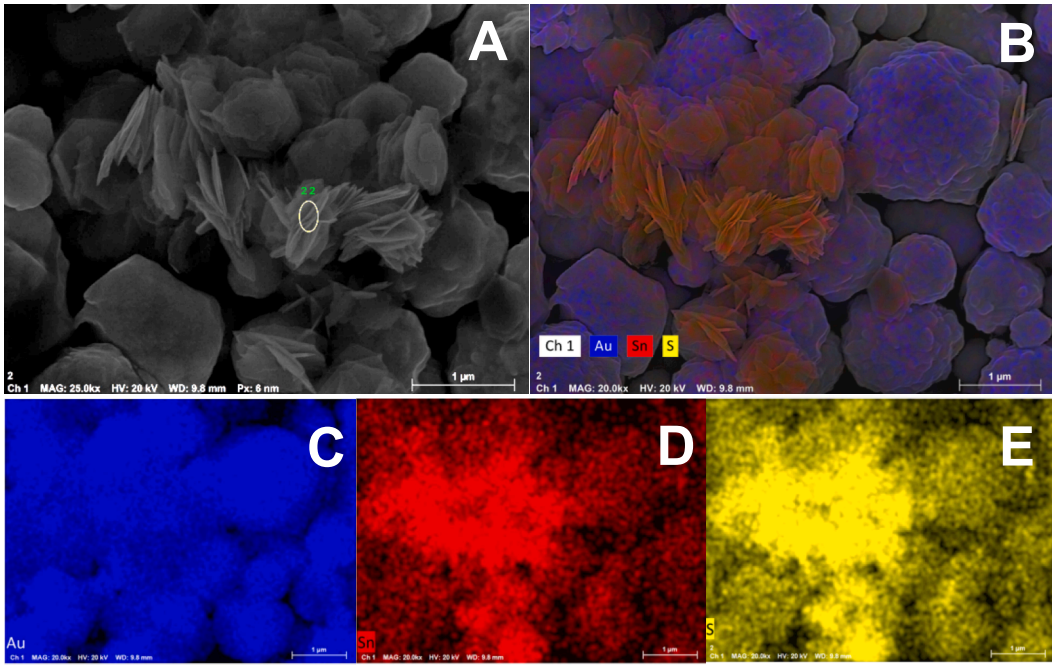

Fig. 3. SEM-EDX images of the SnS_2/SPAuE. A) Image of the area corresponding to the EDX spectrum of the SnS_2/SPAuE. Elemental map of B) SnS_2/SPAuE, C) gold, D) tin and E) sulfur.

3.4. Optimization of experimental variables

To study the electrochemiluminescent response of the platform and to establish the optimal conditions, different concentrations of SnS_2 (0.050 mg/mL, 0.10 mg/mL, and 0.25 mg/mL) were prepared in EtOH and the electrodes were modified by drop casting with 3 μL of each one of them. Fig. 4 shows that the maximum electrochemiluminescent signal was obtained at a concentration of 0.10 mg/mL, since, at concentrations higher or lower than this, the electrochemiluminescent signal decreased. The raw data are presented in Fig. S9. These results may be explained by an improvement of the electron transfer when the amount of deposited SnS_2 increases until an optimum, then it decreases when the semiconductor layer that covers the electrode becomes too thick. It may also be due to the fact that increasing the amount of SnS_2 on the electrode surface produces a greater scattering of light and decreases the electrochemiluminescent response. This effect has also been observed on other semiconductor-modified surfaces [32,35]. Therefore, 0.10 mg/mL was selected as the optimal concentration of SnS_2 for all subsequent experiments.

Semiconductor materials are currently being used for the functionalization of electrodes for the development of electrochemiluminescent sensors [36,37,43–47]. Furthermore, a new trend is the mixture of different nanomaterials. However, only in some results and situations does this mixture of nanomaterials of different nature show their synergistic character [32,48–50]. For this reason, the results obtained in the electrochemiluminescent response using different conductive metallic nanoparticles and the combination with the semiconductor SnS_2 are shown below.

In order to study the behavior of metallic nanoparticles in the electrochemiluminescent response, the electrode was modified with commercial AgNPs and AuNPs synthesized as described in Procedures. To determine which metallic nanoparticles provided a higher ΔECL, the SPAuE was modified with different volumes of each of the solutions (5, 10 and 15 μL) by drop casting. Fig. S10B shows that the use of 5 μL of AuNPs gave rise to the highest ΔECL, so this volume of AuNPs was selected as optimal and the AgNPs were discarded.

With the purpose of studying whether both nanomaterials had a synergistic effect on the ECL response, AuNPs were combined with SnS_2. To do this, a concentration of 0.1 mg/mL SnS_2 was deposited on the surface of the SPAuE, followed by the AuNPs. Different volumes of SnS_2 (3, 5, 10, 15, 20 and 25 μL) were added followed by 5 μL of AuNPs, both by drop casting (Fig. S11). It was observed that the combination of both nanomaterials, AuNPs and SnS_2, did not produce a synergistic effect since the electrochemiluminescent response decreased compared to that obtained for the electrode modified only with SnS_2 (Fig. 4). This fact could be attributed to the increase in the thickness of the layer of nanomaterials deposited on the electrode surface produces a decrease in electronic exchange. Also, it may be due to the distance at which the semiconductor layer is located from the metal nanoparticles, since when the metal nanoparticles are close to each other, the hybridization plasma of surface plasmon resonance on the surface of the metal nanoparticles and gap plasma resonance between the metallic nanoparticles exhibit higher electromagnetic field intensity and surface plasmon coupling effect than a single conventional AuNPs [51]. For this reason, AuNPs were discarded and only SnS_2 was selected for the modification of SPAuE.

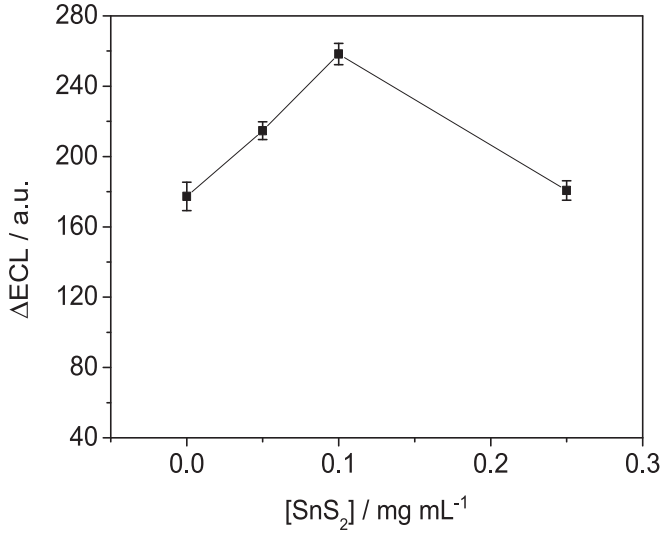

Fig. 4. A) ΔECL response *versus* SnS_2 concentration deposited on SPAuE for a 2 mM $[Ru(bpy)_3]^{2+}$ solution and a mixed solution containing 2 mM $[Ru(bpy)_3]^{2+}$ and 500 μM citrulline, both in 0.1 M PB, pH 8.0. Number of replicate measurements, n = 3. A cyclic sweep was performed between 0 and 1.5 V at 50 mV/s.

Once the optimal conditions for nanostructuring the electrode surface with SnS_2 were selected, the pH, the luminophore concentration and the scan rate were optimized.

First, the pH study was carried out. For this, the electrochemiluminescent response of a solution of 2 mM $[Ru(bpy)_3]^{2+}$ and 500 μM citrulline in 0.1 M PB was measured at different pH (6.0, 7.0, 8.0 and 9.0). To study the luminophore concentration, a 4 mM $[Ru(bpy)_3]^{2+}$ solution was prepared, from which dilutions were made at different concentrations. The same protocol as in the pH study was followed to record the electrochemiluminescent response of the solution of $[Ru(bpy)_3]^{2+}$ and 500 μM citrulline. The luminophore concentrations studied were: 4, 3, 2 and 1 mM. Finally, the scan rate was optimized, performing cyclic potential sweeps at different rates: 2.5, 5, 10, 15, 20, 30 and 50 mV/s.

Fig. S12 shows the electrochemiluminescent responses obtained under the different conditions studied. The electrochemiluminescent signal is maximum when the pH is 8.0 (Fig. S12A) and the concentration of $[Ru(bpy)_3]^{2+}$ is 3.0 mM (Fig. S12B). It was observed that at lower scan rate, the ECL signal was higher (Fig. S12C), being maximum at 2.5 mV/s. The raw electrochemiluminescent data are shown in Fig. S12D–F. In addition to an increase in the electrochemiluminescent signal, the shortest possible measure time is desired to develop an efficient sensor. Since a measurement made at 2.5 mV/s lasts 25 min, the observed increase in the electrochemiluminescent signal at this rate was not sufficient to select it as optimal parameter. For this reason, 15 mV/s was taken as the optimal scan rate since there is a balance between the measurement time (around 3 min) and the improvement of the electrochemiluminescent response.

Accordingly, all subsequent experiments were performed at 15 mV/s on a solution of 3 mM $[Ru(bpy)_3]^{2+}$ in 0.1 M PB, pH 8.0.

3.5. Analytical performance of citrulline ECL-sensor

Once the measurement parameters were optimized, the relationship of the electrochemiluminescent signal as a function of the citrulline concentration was studied. To do this, cyclic potential sweeps were performed from 0 to 1.5 V at 15 mV/s on a mixed solution of 3 mM $[Ru(bpy)_3]^{2+}$ and citrulline with different concentrations in 0.1 M PB, pH 8.0.

The electrochemiluminescent signal was observed to increase linearly ($R^2 = 0.998$) with citrulline concentration in the range from 10.0 μM to 1 mM. This result confirms that ECL can be used as citrulline quantification method. The calibration curve presents a sensitivity of (0.53 ± 0.01) (u.a. μM^{-1}), obtained from the slope, and an ordinate at the origin of (8.31 ± 2.8) (u.a.) (Fig. 5). The analytical parameters were calculated and a detection limit (LOD) of 2.95 μM and a quantification limit (LOQ) of 9.83 μM were obtained. The relative standard deviation (% RDS) was calculated from the values of the standard deviation and the mean of the data, and the value obtained was 4.43 %, indicating considerable reproducibility.

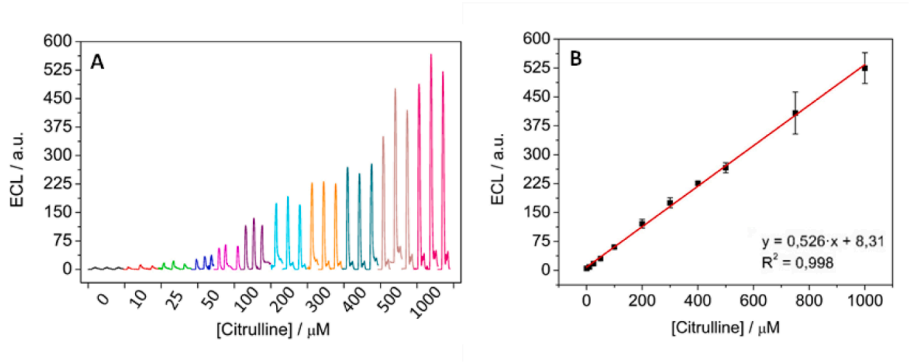

Fig. 5. A) ECL sensor responses as a function of increasing citrulline concentration at SPAuE/SnS_2. B) Calibration curve of the electrochemiluminescent signal for citrulline concentration in the 10.0 μM–1 mM range. Each point is the mean of three measurements on three different electrodes in a solution of 3 mM $[Ru(bpy)_3]^{2+}$ and the corresponding concentration of citrulline in 0.1 M PB, pH 8.0 at 15 mV/s scan rate.

Table 1 shows the analytical parameters previously reported for the determination of citrulline in watermelon samples by other methods. The LOD and LOQ of the sensor developed in this work do not differ significantly from those of the HPLC-based methods. The proposed electrochemiluminescent sensor presents one of the lowest LOD and LOQ while being the simplest method.

The stability of the developed sensor was evaluated by performing ten consecutive electrochemiluminescent measurements on the same electrode (SnS_2/SPAuE) in the presence of 3 mM $[Ru(bpy)_3]^{2+}$ and 100 μM citrulline in 0.1 M PB, pH 8.0. The electrochemiluminescent signal remains constant after ten consecutive measurements (see Fig. S13). From the results it can be concluded that the surface of the SPAuE modified with SnS_2 is stable and it is possible to perform several consecutive measurements on the same platform without observing significant changes in the electrochemiluminescent signal. After consecutives 10 cycles, the sensor kept 96 % of its initial response. To establish the efficiency of the developed electrochemiluminescent sensor, a study of its storage stability over time was carried out. For this, the ECL emission in presence of $[Ru(bpy)_3]^{2+}$ was recorded on the same electrode, modified with 5 μL of SnS_2 in EtOH by drop casting and stored at 4 °C, at different times for 8 days. After this period, it lost only 3 % of its initial response.

The selectivity of the proposed sensor against different potential interfering compounds was studied. Citrulline has been shown to act as a co-reactant due to the groups that make up its chemical structure. It is expected that molecules such as ascorbic acid, glycine, cysteine, arginine, fructose or ornithine may also act as co-reactants, so they have been studied as potential interferents. Also, the presence of potassium and calcium were studied by adding KCl and $CaCl_2$ salts (Fig. S14). In addition, in order to know the ECL response to the potential interferents, measurements were performed for solutions containing: a) all the interfering compound studied at a concentration of 100 μM of each interferent in 0.1 M PBS, pH 8.0 (Fig. S15) and 3 mM $[Ru(bpy)_3]^{2+}$ and b) 3 mM $[Ru(bpy)_3]^{2+}$, 100 μM citrulline and 100 μM interferent in 0.1 M PBS, pH 8.0. We observed that there is no interaction between the interfering compounds that gives rise to an additional increase in electrochemiluminescence signal.

As expected, ascorbic acid increases the electrochemiluminescent signal with respect to the signal obtained for citrulline alone, as well as arginine and ornithine, while the rest of the studied compounds do not produce a significant interference in the electrochemiluminescent response. Ascorbic acid (Vitamin C) is one of the major components of watermelon, which is the main source of citrulline. Arginine and ornithine are compounds involved in some metabolic pathway, however, both compounds do not coexist in foods. It would be very interesting to study ways to solve the effect of this interferent when using the sensor in this type of samples.

The presence of ascorbic acid, ornithine and arginine interferes for the concentrations studied because the variation in the initial analytical signal is greater than 10 %. The maximum allowed concentration values of the interfering compounds for the determination of 100 μM citrulline can be found in Table S1.

3.6. Determination of citrulline in food samples

The applicability of the developed electrochemiluminescent sensor was studied on a watermelon sample. After the extraction process and through standard additions of citrulline, a citrulline concentration of 685 ppm was determined in the sample close to the rind and 494 ppm in the heart area of the watermelon. To validate the result obtained by ECL, the watermelon samples were further analyzed by high performance liquid chromatography (HPLC) as a comparative method. The results are shown in Table 2. The average value of citrulline concentration obtained with our method agrees well with that obtained by HPLC, demonstrating that the developed ECL sensor can be used for the determination of citrulline in food samples.

4. Conclusions

An electrochemiluminescent sensor has been developed to determine an amino acid that is involved in many metabolic processes and several foods are present, such as citrulline.

Citrulline has been able to act as a co-reactant, in addition to being the analyte. This fact eliminates the need to find a co-reactant different from the analyte that does not interfere with its signal. Also, by not requiring any prior treatment of the analyte, this becomes a simple experimental system that provides results in a short time.

Table 1
Comparative table of previous methods for the determination of citrulline in watermelon.

Method	LOD (μM)	LOQ (μM)	R^2	Reference
ECL (SPAuE/SnS_2)	2.95	9.83	0.998	This work
RP-HPLC	2.39	7.31	0.996	[52]
HPLC-UV	3.60	12.16	0.995	[53]
1H-RMN	216.91	405.27	0.99	[54]

Table 2
Determination of citrulline in different samples with ECL sensor and with high performance liquid chromatography (HPLC) (n = 3).

Watermelon Sample	Citrulline content/ppm	
	Developed ECL sensor	HPLC
Rind sample	494 ± 9	565 ± 6
Flesh sample	685 ± 9	580 ± 6

The semiconductor nanomaterial SnS_2 has been synthesized with the aim of nanostructuring disposable gold screen printed electrodes to amplify the electrochemiluminescence response in the presence of $[Ru(bpy)_3]^{2+}$. The platform has been characterized using different techniques such as: SEM, TEM and DLS, determining its quality as a nanomaterial in the form of hexagonal crystals. In addition, through electrical impedance spectroscopy.

The developed electrochemiluminescent sensor allows the determination of citrulline up to a concentration of 10 μM, with the detection and quantification limits obtained being 2.95 μM and 9.83 μM, respectively.

Finally, citrulline was determined directly in watermelon, obtaining a concentration of 685 ppm in the area close to the rind and 494 ppm in the heart area of the watermelon and its applicability to determine citrulline in watermelon has been tested with results in good agreement with those obtained by HPLC.

CRediT authorship contribution statement

Claudia Martínez-Asenjo: Investigation. **Marcos Pita:** Writing – original draft, Funding acquisition. **Antonio L. De Lacey:** Writing – original draft, Funding acquisition. **Cristina Gutiérrez-Sánchez:** Writing – original draft, Supervision, Funding acquisition, Conceptualization. **Encarnación Lorenzo:** Writing – original draft, Funding acquisition.

Declaration of competing interest

The authors declare that they have no known competing financial interests or personal relationships that could have appeared to influence the work reported in this paper.

Acknowledgments

This work has been supported the Comunidad Autónoma de Madrid SI3/PJI/2021-00341 and this work has also been supported by the Spanish Ministerio de Ciencia e Innovación (PID2022-142262OA-I00, PID2020-116728-RB100 and TED2021-129738B-I00). M.P. and A.L.D. L. acknowledge the PID2021-1241160B-I00 "ELECTROSYSCAT" project funded by MCIN/AEI/ 10.13039/501100011033 and by the European Union. The authors thank Tamara Guerrero-Esteban for her additional work.

Appendix A. Supplementary data

Supplementary data to this article can be found online at https://doi.org/10.1016/j.microc.2024.111939.

Data availability

Data will be made available on request.

References

[1] S. Bahri, N. Zerrouk, C. Aussel, C. Moinard, P. Crenn, E. Curis, J.-C. Chaumeil, L. Cynober, S. Sfar, Nutrition 29 (2013) 479–484.
[2] P. Crenn, B. Messing, L. Cynober, Clin. Nutr. 27 (2008) 328–339.
[3] E. Curis, I. Nicolis, C. Moinard, S. Osowska, N. Zerrouk, S. Bénazeth, L. Cynober, Amino Acids 29 (2005) 177–205.
[4] S. Osowska, T. Duchemann, S. Walrand, A. Paillard, Y. Boirie, L. Cynober, C. Moinard, Am. J. Physiol.-Endocrinol. Metab. 291 (2006) E582–E586.
[5] A. Martínez-Sánchez, F. Alacid, J.A. Rubio-Arias, B. Fernández-Lobato, D.J. Ramos-Campo, E. Aguayo, J. Agric. Food Chem. 65 (2017) 4395–4404.
[6] M.S. Mirenayat, S. Moradi, H. Mohammadi, M.H. Rouhani, Curr. Hypertens. Rep. 20 (2018) 98.
[7] V. Joshi, A.R. Fernie, Amino Acids 49 (2017) 1543–1559.
[8] B. Walton, G. Jackson, N. Deutz, G. Cote, J. Biomed. Opt. 22 (2017) 075002.
[9] A.D. Gill, B.L. Hickey, S. Wang, M. Xue, W. Zhong, R.J. Hooley, Chem. Commun. 55 (2019) 13259–13262.
[10] H. Chen, H. Zhao, L. Xiang, H. Wu, Y. Liang, X.-A. Huang, J. Zhang, Org. Biomol. Chem. 18 (2020) 5120–5124.
[11] R. Lavanya, V. Srinivasadesikan, M.-C. Lin, V. Padmini, J. Mol. Struct. 1288 (2023) 135771.
[12] Y. Deng, R. Chen, T. Hu, J. Yao, J. Wang, Food Anal. Methods 10 (2017) 1369–1376.
[13] S. Wang, M. Zhou, Y. Zhu, B. Peng, J. Yang, Y. Ma, J. Electrochem. Soc. 167 (2020) 086508.
[14] Y. Zhao, L. Bouffier, G. Xu, G. Loget, N. Sojic, Chem. Sci. 13 (2022) 2528–2550.
[15] M.M. Richter, Chem. Rev. 104 (2004) 3003–3036.
[16] W. Miao, in: Handbook of Electrochemistry, Elsevier, Amsterdam, 2007, pp. 541–590.
[17] S. O'Connor, L. Dennany, E. O'Reilly, Bioelectrochemistry 149 (2023) 108286.
[18] T. Guerrero-Esteban, C. Gutiérrez-Sánchez, A.M. Villa-Manso, M. Revenga-Parra, F. Pariente, E. Lorenzo, Talanta 247 (2022) 123543.
[19] T. Guerrero-Esteban, C. Gutiérrez-Sánchez, E. Martínez-Periñán, M. Revenga-Parra, F. Pariente, E. Lorenzo, Sens. Actuators B 330 (2021) 129389.
[20] C. Gutiérrez-Sánchez, M. Mediavilla, T. Guerrero-Esteban, M. Revenga-Parra, F. Pariente, E. Lorenzo, Carbon 159 (2020) 303–310.
[21] T. Guerrero-Esteban, C. Gutiérrez-Sánchez, T. García-Mendiola, M. Revenga-Parra, F. Pariente, E. Lorenzo, Sens. Actuators B 343 (2021) 130096.
[22] C. Padmakumari Kurup, S. Abdullah Lim, M.U. Ahmed, Bioelectrochemistry 147 (2022) 108170.
[23] A. Fiorani, J.P. Merino, A. Zanut, A. Criado, G. Valenti, M. Prato, F. Paolucci, Curr. Opin. Electrochem. 16 (2019) 66–74.
[24] A. Abbas, H.M.A. Amin, Microchem. J. 175 (2022) 107166.
[25] F. Lou, X. Xie, Q. Li, Y. Wang, Q. Li, J. Electroanal. Chem. 888 (2021) 115166.
[26] L. Wang, Y. Liu, J. Yan, H. Li, Y. Tu, ACS Sens. 8 (2023) 2859–2868.
[27] D. Hong, K. Kim, E.-J. Jo, M.-G. Kim, Anal. Chem. 93 (2021) 7925–7932.
[28] Y. Liu, Y. Nie, M. Wang, Q. Zhang, Q. Ma, Biosens. Bioelectron. 148 (2020) 111823.
[29] G.B. Grad, E.R. González, J. Torres-Díaz, E.V. Bonzi, J. Phys. Chem. Solid 168 (2022) 110788.
[30] Z. Cao, Y. Shu, H. Qin, B. Su, X. Peng, ACS Cent. Sci. 6 (2020) 1129–1137.
[31] E. Yang, Y. Zhang, Y. Shen, Anal. Chim. Acta 1209 (2022) 339140.
[32] T. Guerrero-Esteban, B.L. Sánchez, L. Expósito, D. Rodríguez-San-Miguel, F. Zamora, F. Pariente, C. Gutiérrez-Sánchez, E. Lorenzo, Sens. Actuators B 396 (2023) 134649.
[33] M. Zhou, Y. Pu, Q. Wu, P. Wang, T. Liu, M. Zhang, Sens. Actuators B 319 (2020) 128298.
[34] C. Jarne, L. Paul, J.C. Conesa, S. Shleev, A.L. De Lacey, M. Pita, ChemElectroChem 6 (2019) 2755–2761.
[35] T. Guerrero-Esteban, C. Gutiérrez-Sánchez, M. Revenga-Parra, J.L. Pau, F. Pariente, E. Lorenzo, Talanta 204 (2019) 63–69.
[36] S. Li, Y. Deng, C. Pang, X. Ma, Y. Wu, M. Wang, J. Li, Z. Xu, L. Zhang, Sens. Actuators B 394 (2023) 134415.
[37] Y. Guo, Y. Nie, P. Wang, Z. Li, Q. Ma, Talanta 259 (2023) 124559.
[38] G. Kiruthigaa, C. Manoharan, C. Raju, J. Jayabharathi, S. Dhanapandian, Spectrochim. Acta A Mol. Biomol. Spectrosc. 129 (2014) 415–420.
[39] R. Lucena, F. Fresno, J.C. Conesa, Appl. Catal. A 415–416 (2012) 111–117.
[40] A. Chakrabarti, J. Lu, A.M. McNamara, L.M. Kuta, S.M. Stanley, Z. Xiao, J. A. Maguire, N.S. Hosmane, Inorg. Chim. Acta 374 (2011) 627–631.
[41] S. Bhattacharjee, J. Control. Release 235 (2016) 337–351.
[42] G. Su, V.G. Hadjiev, P.E. Loya, J. Zhang, S. Lei, S. Maharjan, P. Dong, P.M. Ajayan, J. Lou, H. Peng, Nano Lett. 15 (2015) 506–513.
[43] M. Li, Z. Li, P. Wang, Q. Ma, Biosens. Bioelectron. 228 (2023) 115225.
[44] X. Zhang, P. Wang, Z. Liang, W. Zhong, Q. Ma, Talanta 266 (2024) 124952.
[45] Z. Li, P. Wang, Z. Liang, D. Wang, Y. Nie, Q. Ma, Anal. Chem. 95 (2023) 9706–9713.
[46] Y. Lin, J. Wu, X. Tan, K. Huang, Sens. Actuators B 382 (2023) 133541.
[47] M. Zhang, Q. Kong, J. Huang, Y. Xiang, G. Wang, J. Han, Y. Guo, S. Zhao, X. Sun, Sens. Actuators B 361 (2022) 131690.
[48] J. Wen, D. Jiang, X. Shan, W. Wang, F. Xu, Z. Chen, Analyst 146 (2021) 3493–3499.
[49] Y. Nie, Z. Liang, P. Wang, Q. Ma, X. Su, Anal. Chem. 93 (2021) 17086–17093.
[50] Q. Feng, L. Qin, B. Dou, X. Han, P. Wang, ACS Appl. Nano Mater. 5 (2022) 16325–16331.
[51] Y. Shan, J.-J. Xu, H.-Y. Chen, Chem. Commun. (2009) 905–907.
[52] R. Ridwan, H.R. Abdul Razak, M.I. Adenan, W.M. Md Saad, Int. J. Anal. Chem. 2018 (2018) 4798530.
[53] J.B. Johnson, B. Ohri, K.B. Walsh, M. Naiker, Food Anal. Methods 15 (2022) 104–114.
[54] G.K. Jayaprakasha, B.S. Patil, Talanta 153 (2016) 268–277.